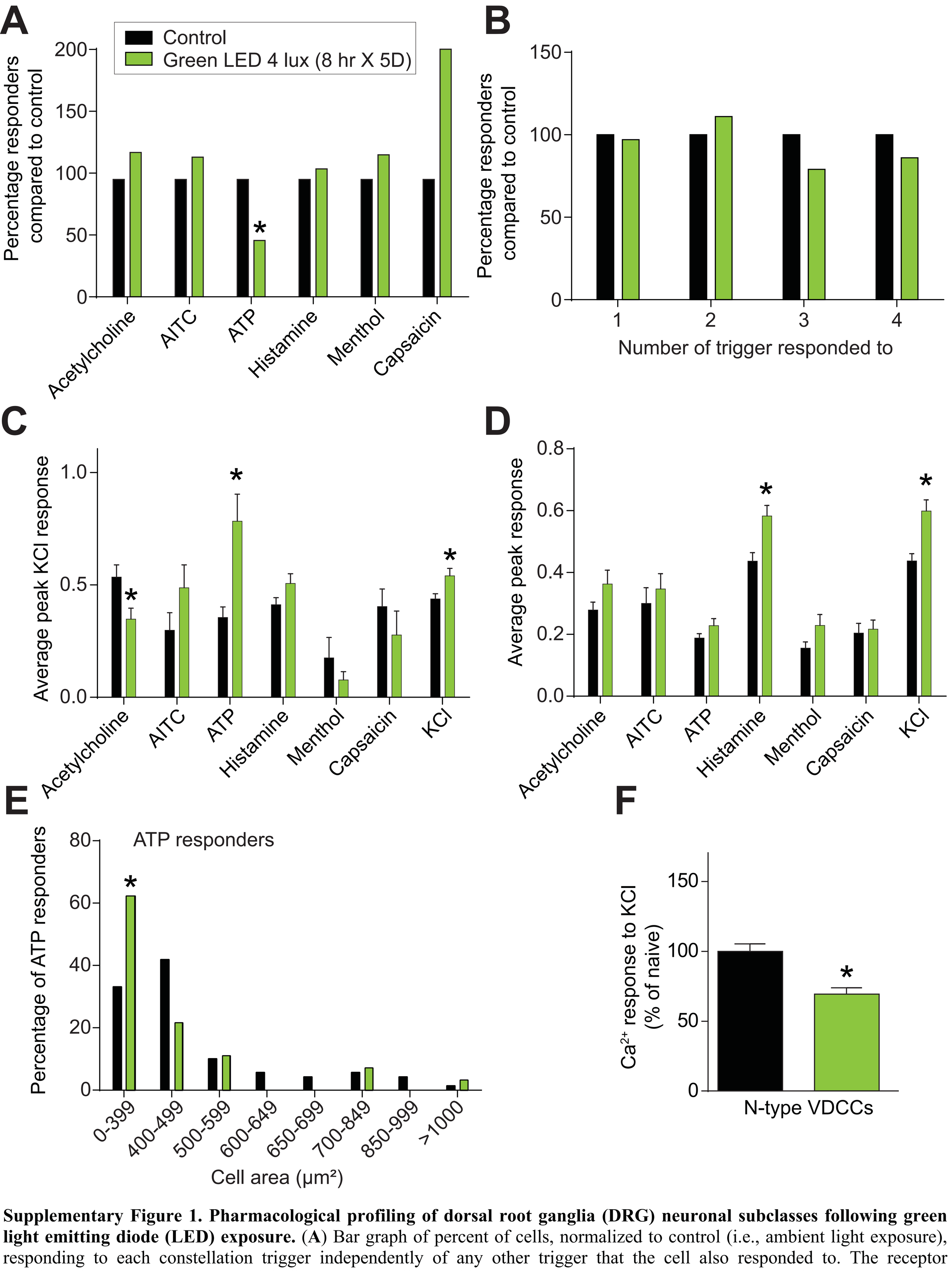

Supplementary Figure 1. Pharmacological profiling of dorsal root ganglia (DRG) neuronal subclasses following green light emitting diode (LED) exposure. (**A**) Bar graph of percent of cells, normalized to control (i.e., ambient light exposure), responding to each constellation trigger independently of any other trigger that the cell also responded to. The receptor agonists/triggers used were: acetylcholine (1 mM), allyl isothiocyanate (AITC; 200 μM), ATP (10 μM), histamine (50 μM), menthol (400 nM), or capsaicin (100 nM). All cells were selected based on their response to a depolarizing pulse of KCl (90 mM). Sensory neurons from GLED exposed rats had a decreased proportion of cells responding to ATP (z-test). (**B**) The response of DRG neurons to one or more receptor agonist was analyzed. The bar graph indicates the percentage of cells, normalized to control conditions, which responded to the indicated number of triggers. The number 1 corresponds to the proportion of cells that responded to KCl only and no other trigger. No significant change was observed in each category of cells between control condition and GLED exposure. (**C**) Bar graph of average peak KCl response in different functional neuronal populations defined by their response to indicated receptor agonist. Sensory neurons from GLED exposed rats, showed a decreased response to KCl among the acetylcholine-sensitive neurons and an increased response to KCl in the ATP-sensitive neurons (*$p<0.05$; one-way ANOVA). (**D**) Bar graph of average peak calcium response elicited by each receptor agonist in DRG neurons prepared from GLED exposed or control rats. Significant increases in average peak response for histamine and KCl were observed (*$p<0.05$; one-way ANOVA). (**E**) Bar graphs of sizes of neurons responding to ATP. Data are from 2 independent experiments with a total n=186 cells from control rats and n=161 from GLED exposed rats. (**F**) Bar graph of the normalized peak fluorescence response of DRGs prepared from GLED exposed or control rats in the presence of pharmacological blockers (see Methods for details) specific for the indicated calcium channel subtypes. Values represent the average ± S.E.M., n=71–206 cells per condition. Asterisks indicate statistical significance compared with DRGs from ambient light exposed rats (i.e., control)($p<0.05$, Student's t-test).

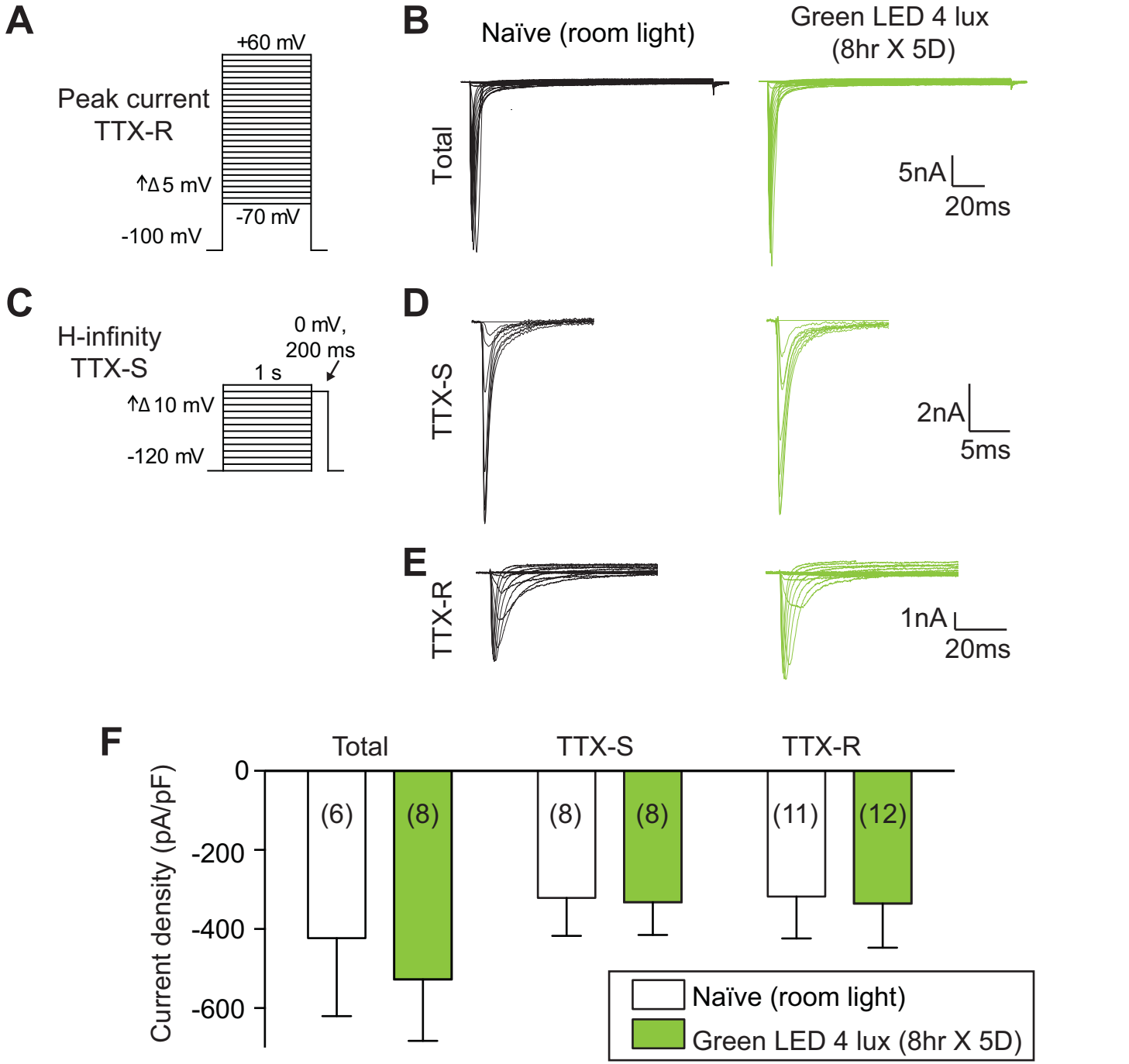

Supplementary Figure 2. Voltage-gated sodium currents in rat dorsal root ganglia (DRG) neurons are not affected by green light emitting diode (GLED) exposure. (**A**) Voltage protocol used to evoke tetrodotoxin-resistant (TTX-R) Na^+ currents. (**B**) Representative family of total Na^+ currents in DRG neurons from naïve and green LED exposed rats. (**C**) Voltage protocol used to evoke tetrodotoxin-sensitive (TTX-S) Na^+ currents. Representative family of TTX-S (**D**) and TTX-R (**E**) Na^+ currents in DRG neurons from naïve and green LED exposed rats. (**F**) Summary of the peak current density (pA/pF) from DRG neurons (n=6–12 as indicated in parentheses within the bars) cultured from either naïve or green LED exposed rats. No significant difference was observed for total, TTX-S or TTX-R Na^+ current between naïve and GLED treatment ($p>0.05$, Student's t test).

Supplementary Methods

1. Primary dorsal root ganglion (DRG) neuronal cultures.

Sensory DRG neurons from Sprague-Dawley rats were isolated as described previously [2; 4]. Dorsal root ganglia (from thoracic 2 to lumbar 6 spinal levels) were excised aseptically and placed in Hank buffered salt solution (HBSS, Life technologies) containing penicillin (100 U/mL) and streptomycin (100 µg/mL, Cat# 15140, Life technologies) on ice. The ganglia were dissociated enzymatically by a 45 min incubation (37°C) in a DMEM (Cat# 11965, Life technologies) solution containing neutral protease (3.125 $mg.ml^{-1}$, Cat#LS02104, Worthington) and collagenase Type I (5 $mg.ml^{-1}$, Cat# LS004194, Worthington). The dissociated cells were resuspended in complete DRG medium, DMEM containing penicillin (100 U/mL), streptomycin (100 µg/mL), 30 $ng.ml^{-1}$ nerve growth factor and 10% fetal bovine serum (Hyclone). For Ca^{2+} imaging, the cells were seeded on poly-D-lysine (Cat# P6407, Sigma) coated glass coverslips (Cat# 72196-15, electron microscopy sciences) as a drop of 20 µl on the center of each coverslip, then placed in a 37°C, 5 % CO_2 incubator for 45–60 min to allow cells to attach. Then the cultures were flooded by gently adding complete DRG medium on the edge of each well to avoid detaching any weakly adherent cell.

2. Calcium imaging.

DRG neurons were loaded at 37°C with 3µM Fura-2AM (Cat#F-1221, Life technologies, stock solution prepared at 1mM in DMSO, 0.02% pluronic acid, (Cat#P-3000MP, Life technologies) for 30 minutes (K_d= 25µM, λ_{ex} 340, 380 nm/λ_{emi} 512 nm) to follow changes in intracellular calcium ($[Ca^{2+}]_c$) in Tyrode's solution (at ~310 mOsm) containing 119 mM NaCl, 2.5mM KCl, 2mM $MgCl_2$, 2mM $CaCl_2$, 25mM HEPES, pH 7.4 and 30mM glucose. All calcium-imaging experiments were done at room temperature (~23°C). Fluorescence imaging was performed with an inverted microscope, Nikon Eclipse T*i*-U (Nikon Instruments Inc.), using objective Nikon Super Fluor MTB FLUOR 10x 0.50 and a Photometrics cooled CCD camera CoolSNAP ES^2 (Roper Scientific) controlled by NIS Elements software (version 4.20, Nikon instruments). The excitation light was delivered by a Lambda-LS system (Sutter Instruments). The excitation filters (340±5 nm and 380±7 nm) were controlled by a Lambda 10-2 optical filter change (Sutter Instruments). Fluorescence was recorded through a 505 nm dichroic mirror at 535±25 nm. To minimize photobleaching and phototoxicity, the images were taken every 10 seconds during the time-course of the experiment using the minimal exposure time that provided acceptable image quality. The changes in $[Ca^{2+}]_c$ were monitored by following the ratio of F_{340}/F_{380}, calculated after subtracting the background from both channels.

3. Pharmacological profiling of sensory neurons.

After a 1-minute baseline measurement, Ca^{2+} influx was stimulated by the addition of the following receptor agonists, in order: 1 mM acetylcholine (Ach), 200 µM allyl isothiocyanate (AITC), 10 µM adenosine triphosphate (ATP), 50 µM histamine, 400 nM menthol and 100 nM capsaicin diluted in Tyrode's solution. At the end of the pharmacological profiling protocol, cell viability was assessed by depolarization-induced Ca^{2+} influx using and an excitatory KCl solution comprised of 32mM NaCl, 90mM KCl, 2mM $MgCl_2$, 2mM $CaCl_2$, 25mM HEPES, pH 7.4, 30mM glucose. After the 1-minute baseline measurement, each trigger was applied for 15-seconds in the order indicated above in 2-minutes intervals. Following each trigger, bath solution was continuously perfused over the cells to wash off excess of the trigger and to let the sensory neurons return to baseline. This process was automated using the software WinTask x64 (Version 5.1, WinTask) that controlled the perfusion of the standard bath solution and triggers through Valvelink 8.2 software (Automate Scientific). A cell was defined as a 'responder' if its fluorescence ratio of F_{340}/F_{380} was greater than 10% of the baseline value calculated using the average fluorescence in the 30 seconds preceding application of the trigger.

To isolate N-type (i.e., CaV2.2) voltage-dependent calcium channel (VDCC), cells were incubated during the 30 min Fura2-AM loading step with the following drugs to inhibit the other subtypes present in these cells: (all purchased from Alomone labs, Jerusalem, Israel) nifedipine (10 µM, L-type), SNX-482 (200 nM, R-type)[10], ω-agatoxin TK (200 nM, P/Q-type)[8] and 3,5-dichloro-N-(1-[2,2-dimethyl-tetrahydro-pyran-4-ylmethyl]-4-fluoro-piperidin-4-ylmethyl)-benzamide (TTA-P2, 1 µM, T-type)[3].

4. Whole-cell voltage clamp electrophysiology.

Whole cell voltage clamp recordings were performed at room temperature using an EPC 10 Amplifier-HEKA as previously described [4]. The internal solution for voltage clamp recordings of DRG cells contained (in mM): 140 CsF, 1.1 Cs-EGTA, 10 NaCl, and 15 HEPES (pH 7.3, 290–310 mOsm/L) and the external solution contained (in mM): 140 NaCl, 3 KCl, 30 tetraethylammonium chloride, 1 $CaCl_2$, 0.5 $CdCl_2$, 1 $MgCl_2$, 10 D-glucose, 10 HEPES (pH 7.3, 310–315 mosM/L). Electrodes were pulled from standard wall borosilicate glass capillaries from Warner Instruments with a P-97 electrode puller from Sutter Instruments and heat polished to final resistances of 1.5-3 megaOhms when filled with internal solutions. Whole-cell capacitance and series resistance were compensated with linear leak currents were digitally

subtracted by P/4 method for voltage clamp experiments and bridge balance compensated in current clamp experiments. Signals were filtered at 10 kHz and digitized at 10-20 kHz. Cells wherein series resistance or bridge balance was over 15 megaOhm or fluctuated by more than 30% over the course of an experiment were omitted from datasets. Analysis was performed using Fitmaster software from HEKA and Origin9.0 software from OriginLab Corp.

4.1 Voltage clamp protocols.

DRGs were subjected to current-density (I-V) protocol (**Supplementary Figure 2A**) and H-infinity (pre-pulse inactivation protocol)(**Supplementary Figure 2C**). In the I-V protocol, cells were held at a –80 mV holding potential prior to depolarization by 20 ms voltage steps from –70 mV to +60 mV in 5 mV increments. This allowed for collection of current density data to analyze activation of sodium channels as a function of current versus voltage and also peak current density which was typically observed near ~ 0-10 mV and normalized to cell capacitance (pF). To estimate tetrodotoxin-resistant (TTX-R) contributions, the I-V protocol was run after incubation with 500 nM TTX. Following holding at –100 mV, 200 ms voltage steps from –70 mV to +60 mV in 5 mV increments allowed for analysis of peak currents. The TTX-R peak current density was always measured at depolarizations near 0 mV and within 10 ms of the voltage step protocol. Given the previously identified properties of NaV1.8 and NaV1.9 TTX-R currents, this voltage-dependence and activation profile suggests our analysis of peak current density represents only NaV1.8 current [7]. Thus, we analyzed sodium current present at 150 ms following a voltage pulse to –60 mV, an established method of isolating Nav1.9 current.

In the H-infinity protocol, cells were held at –100 mV and subjected to conditioning voltage steps for 1 s varying from –120 mV to 0 mV in 10 mV increments. This conditioning step was followed by a 0 mV test pulse for 200 ms to analyze current. The H-infinity protocol allowed subtraction of electrically isolated TTX-R (current available after -40 mV prepulse) from total current (current available after –120 mV prepulse) to estimate tetrodotoxin-sensitive (TTX-S) current. This protocol is possible due to differential inactivation kinetics of TTX-R versus TTX-S channels wherein TTX-S current becomes activated and then fast-inactivated during the 1s pulse to –40 mV. A visual representation of this protocol is presented in **Supplementary Figure 2C**. For all protocols, a test pulse was performed before and after the voltage protocol to evaluate run-down or run-up of currents during the voltage protocols and to exclude data from cells with currents that were altered as a function of time.

Results

1. Functional 'fingerprinting' of sensory neurons from GLED exposed rats.

To investigate neuronal changes that may have occurred in sensory neurons following GLED exposure, we performed pharmacological profiling of neuronal populations. DRG cultures were prepared from rats after exposure to GLED for eight hours daily for five days and collected immediately after light termination or control conditions and their functional profiling performed with by Ca^{2+} imaging as described recently [9]. This approach allows us to characterize the molecular changes occurring in the sensory neurons after light exposure and may reveal light-induced changes leading to antinociception.

We first analyzed the proportion of sensory neurons responding to each receptor agonist challenge and observed a significant decrease of the proportion of sensory neurons responding to ATP in GLED exposed rats compared to control (**Supplementary Figure 1A**). Although, there is a trend towards an increased percentage of neurons responding to capsaicin, from GLED exposed rats, the change did not reach statistical significance ($p=0.065$ compared with control) (**Supplementary Figure. 1A**). These results suggest that GLED exposure may induce functional changes in ATP signaling in sensory neurons.

We then asked if GLED exposure could alter the overall competence of the sensory neurons to respond to one or more receptor agonist challenges. We did not observe any change of functional competence in sensory neurons isolated from GLED exposed rats compared to rats exposed to ambient light (**Supplementary Figure 1B**), suggesting that the antinociception provided by green light exposure does not arise from a desensitization of the sensory neurons.

Next, to analyze how different types of sensory neurons could be altered by light exposure, we investigated the capacity of sensory neurons to respond to depolarization-induced Ca^{2+} influx as voltage gated Ca^{2+} channel activity has been directly linked to neurotransmitter release [5; 6]. Here, we found that GLED exposure decreased depolarization-induced Ca^{2+} influx in acetylcholine (Ach)-sensitive neurons (**Supplementary Figure 1C**). In contrast, ATP responding neurons, from rats exposed to GLED, had an increased depolarization-induced Ca^{2+} influx (**Supplementary Figure 1C**). Next, we investigated if the Ca^{2+} influx elicited by each receptor agonist varied after GLED exposure. Here, we observed

an increased Ca^{2+} influx triggered by histamine application in neurons prepared from GLED exposed rats (**Supplementary Figure 1D**). We also observed a global increase of the depolarization-induced Ca^{2+} influx in sensory neurons prepared from GLED exposed rats (**Supplementary Figure 1D**).

After having determined that sensory neurons isolated from GLED exposed rats had a decreased capacity to respond to ATP and have a trend toward increased capacity to respond to capsaicin, we next investigated if these changes were due to a specific neuronal population. To do so, we stratified the sensory neuron populations based on their cell surface areas. We could not identify a specific cell population enriched between the capsaicin responding sensory neurons from GLED exposed rats compared to control rats. While we observed a decreased proportion of neurons responding to ATP in the GLED exposed rats, there were significantly more small sized neurons responding to ATP (**Supplementary Figure 1E**). All the other neuronal size subclasses were decreased, but did not reach statistical significance (**Supplementary Figure 1E**). These neurons have an increased response to depolarization-induced Ca^{2+} influx that could result in a greater ability to signal through anti-nociceptive pathways involving ATP. Next, we pharmacologically isolated CaV2.2 Ca^{2+} channel subtype to assess the effects of GLED exposure on this channel previously linked to anitnociception. Ca^{2+} influx via the N-type channel was decreased in GLED exposed rat DRG neurons (**Supplementary Figure 1F**).

2. Characterizing sodium currents in sensory neurons from GLED exposed rats.

The properties of sodium currents have been proposed to be important for neuronal sensitization [1]. Therefore the possible contribution of TTX-R I_{Na} and TTX-S I_{Na} to sensitization was examined. In small diameter sensory neurons, tetrodotoxin (TTX) can be used to separate total I_{Na} into those currents that are sensitive (TTX-S, predominantly NaV1.1 and NaV1.6) and resistant (TTX-R, predominantly NaV1.8) to blockage by this toxin [11]. Representative traces for total, TTX-S, and TTX-R I_{Na} in DRG neurons from ambient (room) light and GLED exposed rats are shown in **Supplementary Figure 2**. None of these currents were changed between the two DRG populations (**Supplementary Figure 2**). Additionally, the voltage dependence for activation of the currents was also nearly the same between the two DRG populations (data not shown). These results suggest that the sodium currents do not contribute to the GLED-induced analgesia.

References

[1] Blair NT, Bean BP. Roles of tetrodotoxin (TTX)-sensitive Na+ current, TTX-resistant Na+ current, and Ca2+ current in the action potentials of nociceptive sensory neurons. The Journal of neuroscience : the official journal of the Society for Neuroscience 2002;22(23):10277-10290.

[2] Brittain JM, Duarte DB, Wilson SM, Zhu W, Ballard C, Johnson PL, Liu N, Xiong W, Ripsch MS, Wang Y, Fehrenbacher JC, Fitz SD, Khanna M, Park CK, Schmutzler BS, Cheon BM, Due MR, Brustovetsky T, Ashpole NM, Hudmon A, Meroueh SO, Hingtgen CM, Brustovetsky N, Ji RR, Hurley JH, Jin X, Shekhar A, Xu XM, Oxford GS, Vasko MR, White FA, Khanna R. Suppression of inflammatory and neuropathic pain by uncoupling CRMP-2 from the presynaptic Ca(2)(+) channel complex. Nature medicine 2011;17(7):822-829.

[3] Choe W, Messinger RB, Leach E, Eckle VS, Obradovic A, Salajegheh R, Jevtovic-Todorovic V, Todorovic SM. TTA-P2 is a potent and selective blocker of T-type calcium channels in rat sensory neurons and a novel antinociceptive agent. Molecular pharmacology 2011;80(5):900-910.

[4] Dustrude ET, Wilson SM, Ju W, Xiao Y, Khanna R. CRMP2 protein SUMOylation modulates NaV1.7 channel trafficking. The Journal of biological chemistry 2013;288(34):24316-24331.

[5] Kress M, Izydorczyk I, Kuhn A. N- and L- but not P/Q-type calcium channels contribute to neuropeptide release from rat skin in vitro. Neuroreport 2001;12(4):867-870.

[6] Maggi CA, Tramontana M, Cecconi R, Santicioli P. Neurochemical evidence for the involvement of N-type calcium channels in transmitter secretion from peripheral endings of sensory nerves in guinea pigs. Neuroscience letters 1990;114(2):203-206.

[7] Maruyama H, Yamamoto M, Matsutomi T, Zheng T, Nakata Y, Wood JN, Ogata N. Electrophysiological characterization of the tetrodotoxin-resistant Na+ channel, Na(v)1.9, in mouse dorsal root ganglion neurons. Pflugers Arch 2004;449(1):76-87.

[8] Mintz IM, Venema VJ, Swiderek KM, Lee TD, Bean BP, Adams ME. P-type calcium channels blocked by the spider toxin omega-Aga-IVA. Nature 1992;355(6363):827-829.

[9] Moutal A, Chew LA, Yang X, Wang Y, Yeon SK, Telemi E, Meroueh S, Park KD, Shrinivasan R, Gilbraith KB, Qu C, Xie JY, Patwardhan A, Vanderah TW, Khanna M, Porreca F, Khanna R. (S)-Lacosamide inhibition of CRMP2 phosphorylation reduces postoperative and neuropathic pain behaviors through distinct classes of sensory neurons identified by constellation pharmacology. Pain 2016.

[10] Newcomb R, Szoke B, Palma A, Wang G, Chen X, Hopkins W, Cong R, Miller J, Urge L, Tarczy-Hornoch K, Loo JA, Dooley DJ, Nadasdi L, Tsien RW, Lemos J, Miljanich G. Selective peptide antagonist of the class E calcium channel from the venom of the tarantula Hysterocrates gigas. Biochemistry 1998;37(44):15353-15362.

[11] Roy ML, Narahashi T. Differential properties of tetrodotoxin-sensitive and tetrodotoxin-resistant sodium channels in rat dorsal root ganglion neurons. The Journal of neuroscience : the official journal of the Society for Neuroscience 1992;12(6):2104-2111.